Chemical Engineering Science 71 (2012) 520–530

Contents lists available at SciVerse ScienceDirect

Chemical Engineering Science

journal homepage: www.elsevier.com/locate/ces

Simulation and control of aggregate surface morphology in a two-stage thin film deposition process for improved light trapping

Jianqiao Huang [a], Gerassimos Orkoulas [a], Panagiotis D. Christofides [a,b,*]

[a] Department of Chemical and Biomolecular Engineering, University of California, Los Angeles, CA 90095, USA
[b] Department of Electrical Engineering, University of California, Los Angeles, CA 90095, USA

ARTICLE INFO

Article history:
Received 11 October 2011
Received in revised form
14 November 2011
Accepted 17 November 2011
Available online 25 November 2011

Keywords:
Materials processing
Thin film solar cells
Mathematical modeling
Systems engineering
Process control
Model predictive control

ABSTRACT

This work focuses on the development of a model predictive control algorithm to simultaneously regulate the aggregate surface slope and roughness of a thin film growth process to optimize thin film light reflectance and transmittance. Specifically, a two-stage thin film deposition process, which involves two microscopic processes: an adsorption process and a migration process, is modeled based on a one-dimensional solid-on-solid square lattice. The first stage of this process utilizes a uniform deposition rate profile to control the thickness of the thin film and the second stage of the process utilizes a spatially distributed deposition rate profile to control the surface morphology of the thin film. Kinetic Monte Carlo (kMC) methods are used to simulate this two-stage thin film deposition process. To characterize the surface morphology and to evaluate the light trapping efficiency of the thin film, aggregate surface roughness and slope corresponding to length scale of visible light are introduced as the root-mean squares of the aggregate surface height profile and aggregate surface slope profile. An Edwards–Wilkinson (EW)-type equation with appropriately computed parameters is used to describe the dynamics of the surface height profile and predict the evolution of the aggregate root-mean-square (RMS) roughness and aggregate RMS slope. A model predictive control algorithm is then developed on the basis of the EW equation model to regulate the aggregate RMS slope and the aggregate RMS roughness at desired levels. Closed-loop simulation results demonstrate the effectiveness of the proposed model predictive control algorithm in successfully regulating the aggregate RMS slope and the aggregate RMS roughness at desired levels that optimize thin film light reflectance and transmittance.

1. Introduction

Thin-film silicon solar cells are currently the most widely used thin film solar cells and an important prospective source of renewable energy. However, an improved conversion efficiency of the solar energy is desired for a wider application of thin-film solar cells. In this direction, research has been conducted on the optical and electrical modeling of thin-film silicon solar cells, which indicates a direct relationship between the light scattering/trapping properties of the thin film interfaces and the conversion efficiencies of thin-film silicon solar cells (Krč et al., 2003; Müller et al., 2004). Recent studies on enhancing thin-film solar cell performance (Zeman and Vanswaaij, 2000; Poruba and Fejfar, 2000; Müller et al., 2004; Springer and Poruba, 2004; Rowlands et al., 2004) have shown that film surface and interface morphology, characterized by aggregate root-mean-square roughness (RMS roughness, r_Δ) and aggregate root-mean-square slope (RMS slope, m_Δ) corresponding to the length scale of visible light (Huang et al., 2011b), play an important role in enhancing absorption of the incident light by the semiconductor layers. Specifically, significant increase of conversion efficiency by introducing appropriately rough interfaces has been reported in several works (Tao and Zeman, 1994; Leblanc and Perrin, 1994; Krč and Zeman, 2002).

Light scattering (Rayleigh scattering) occurs when the incident light goes through a rough interface, where it is divided into four components: specular reflection, specular transmission, diffused reflection and diffused transmission; see Fig. 1 (Tao and Zeman, 1994; Leblanc and Perrin, 1994). If a rough thin film surface is illuminated with a beam of monochromatic light at normal incidence, the total reflectance, R, can be approximately calculated as follows (Davies, 1954):

$$R = R_0 \exp(-4\pi r_\Delta^2/\lambda^2) + R_0 \int_0^{\pi/20} 2\pi^4 \left(\frac{a}{\lambda}\right)^2 \times \left(\frac{r_\Delta}{\lambda}\right)^2 (\cos\theta + 1)^4 \sin\theta \exp[-(\pi a \sin\theta)^2/\lambda^2]\, d\theta \quad (1)$$

* Corresponding author at: Department of Chemical and Biomolecular Engineering, University of California, Los Angeles, CA 90095, USA. Tel.: +1 310 794 1015; fax: +1 310 206 4107.
E-mail address: pdc@seas.ucla.edu (P.D. Christofides).

0009-2509/$ - see front matter © 2011 Elsevier Ltd. All rights reserved.
doi:10.1016/j.ces.2011.11.027

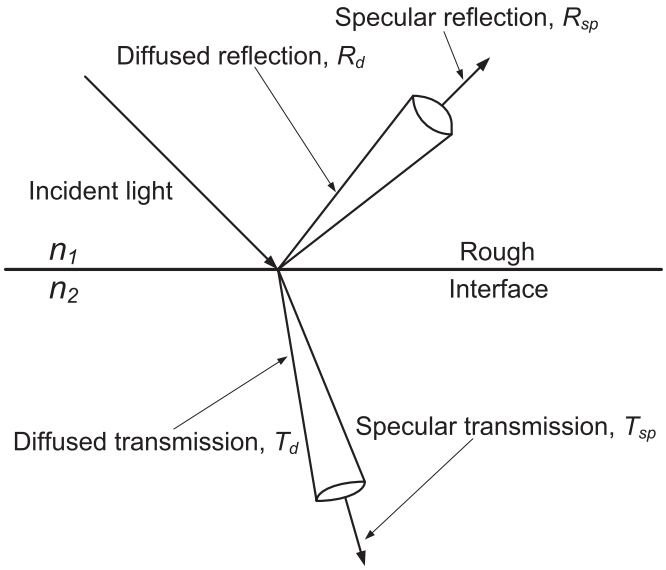

Fig. 1. Light scattering at a rough interface: specular reflection, R_{sp}; diffused reflection, R_d; specular transmission, T_{sp}; and diffused transmission, T_d. n_1 and n_2 are the refractive indices of the two substances above and below the rough interface, respectively.

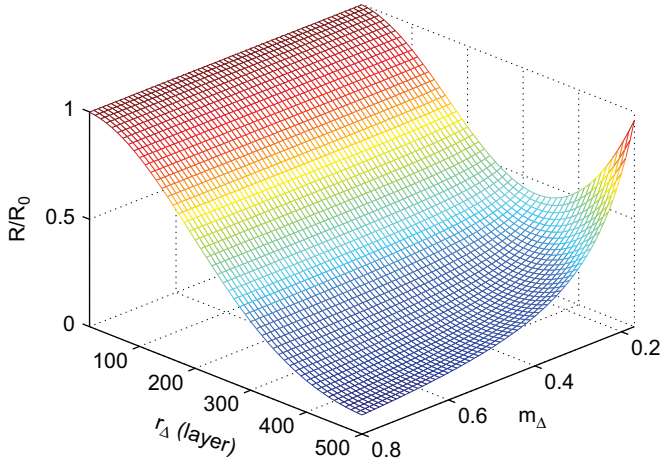

Fig. 2. Reflectance as a function of r_Δ and m_Δ of thin film surface.

where R_0 is the reflectance of a perfectly smooth surface of the same material, r_Δ is the aggregate RMS roughness, Δ is the aggregation size (more discussions about aggregation can be found in Huang et al., 2011b) and in this work $\Delta = 400$, θ is the incident angle, λ is the light wavelength and a is the auto-correlation length of the interface. It can be proved that $a = \sqrt{2} r_\Delta / m_\Delta$, where m_Δ is the aggregate RMS slope of the profile of the interface (Bennett and Porteus, 1961). The numerical integration result of Eq. (1) is shown in Fig. 2. It is necessary to note that Eq. (1) is only valid when θ is small, so in the integration $\theta \in [0, \pi/20]$. From Fig. 2, it can be inferred that both r_Δ and m_Δ strongly influence the intensity of light reflection (and light transmission) at the surface/interface. Specifically, for a thin-film solar cell, the objective is to maximize the light trapping efficiency by controlling the intensities and directions of light reflection and transmission at surfaces and interfaces in the thin film solar cell. This control objective can be achieved by attaining proper values of r_Δ and m_Δ during the thin-film manufacturing process. Therefore, it is important during the manufacturing of thin-film solar cells to regulate process input variables such that the surfaces/interfaces of the produced thin-film solar cells have appropriate values (set-points) of r_Δ and m_Δ that optimize light reflectance and transmittance.

In the context of modeling and control of thin film microstructure and surface morphology, two mathematical modeling approaches have been developed and widely used: kinetic Monte Carlo (kMC) methods and stochastic differential equation (SDE) models. The kMC methods were initially introduced to simulate thin film microscopic processes based on the microscopic rules and the thermodynamic and kinetic parameters obtained from experiments and molecular dynamics simulations (Levine et al., 1998; Zhang et al., 2004; Levine and Clancy, 2000; Christofides et al., 2008). Since kMC models are not available in closed form, they cannot be used for feedback control design and system-level analysis owing to the significant time needed to compute the film surface evolution which renders them inappropriate for real-time control action calculation. On the other hand, SDE models can be derived from the corresponding master equation of the microscopic process and/or identified from process data (Christofides et al., 2008; Hu et al., 2009). The closed form of the SDE models enables their use as the basis for the design of real-time model-based feedback controllers which can regulate thin film surface roughness, film porosity, and film thickness (Hu et al., 2009). Subsequently, the control of aggregate roughness and slope using average deposition rate and amplitude values in the spatially distributed deposition rate profile as manipulated input was studied (Huang et al., 2011b; Zhang et al., 2012). However, feedback control of aggregate surface morphology which also takes film thickness into account and feedback control of aggregate surface morphology using spatially distributed deposition profile of varying complexity have never been studied before.

This work focuses on the development of a model predictive control (MPC) algorithm to simultaneously regulate the aggregate surface slope and roughness of a two-stage thin film growth process to optimize thin film light reflectance and transmittance. In the first stage of the process, a uniform deposition rate profile is utilized and in the second stage of the deposition process, a spatially distributed deposition rate profile is used to carry out the simulation. Initially, a two-stage thin film deposition process is modeled on a one-dimensional solid-on-solid square lattice that involves an adsorption process and a migration process in the microscopic scale using kMC methods. An Edwards–Wilkinson (EW)-type equation (second-order stochastic partial differential equation) is used to describe the dynamics of the aggregate surface height profile obtained form the kMC model and predict the evolution of the aggregate RMS roughness and aggregate RMS slope in a computationally efficient fashion. A model predictive control algorithm is then developed on the basis of the dynamic equation model to regulate the aggregate RMS slope and the aggregate RMS roughness at desired levels. Closed-loop simulation results demonstrate the effectiveness of the proposed model predictive control algorithm in successfully regulating the aggregate RMS slope and the aggregate RMS roughness at desired levels that optimize thin film light reflectance and transmittance.

2. Two-stage thin film deposition process modeling

In this section, an on-lattice kMC model is introduced to simulate the two-stage thin film growth process. Aggregate surface height profile, aggregate RMS roughness, and aggregate RMS slope are defined on the basis of the surface micro-configuration of the thin film. An EW-type equation model is then constructed to describe the dynamics of the surface height profile.

2.1. Two-stage thin film deposition: on-lattice kinetic Monte Carlo model and variable definitions

The two-stage thin film deposition process considered in this work takes place on a one-dimensional solid-on-solid square lattice with periodic boundary conditions (PBCs), as shown in Fig. 3. In this thin film deposition process, two different micro-processes significantly influence the thin film surface morphology (Wang and Clancy, 2001; Yang et al., 1997): an adsorption process and a migration process. In an adsorption process, vertically incident particles are deposited from the gas phase into the thin film. In a migration process, particles on the thin film overcome the energy barriers of the sites and move to neighboring vacant sites with probabilities that obey an Arrhenius-type rate law. In the first state of this deposition process, uniform adsorption rate (in the unit of layer/s) is used to carry out the simulation, i.e.,

$$w(x) = w_{fix} \tag{2}$$

where $x \in [0,L]$ is the position along the lattice, L is the lattice size and in this work $L=40\,000$, and w_{fix} is the uniform adsorption rate in this stage. The simulation time for the first stage of the deposition process is denoted as t_{fix}. In the second stage of this deposition process, a spatially distributed deposition rate profile is utilized, i.e.,

$$w(x) = w_0 + \sum_{i=1}^{m} A_i \sin\left(\frac{2\pi k_i x}{L}\right) \tag{3}$$

where w_0 is the average adsorption rate (in the unit of layer/s), A_i is the amplitude of sine waves and it is requested that $0 \le \sum_{i=1}^{m} A_i \le w_0$ to ensure that $w(x) \ge 0$, $\forall x \in [0,L]$, k_i is the frequency of a sine wave and L is the lattice size. The innovation of introducing the spatially distributed deposition rate profile was introduced in Huang et al. (2011). The average adsorption rate and the amplitude value are the macroscopic variables that can be used as the manipulated variables for control purposes. By introducing the two-stage deposition model, the thickness of the thin film can be manipulated during the first stage and the surface morphology of the thin film can be shaped during the second stage. Throughout this work, Eq. (3) will be used with $m=2$.

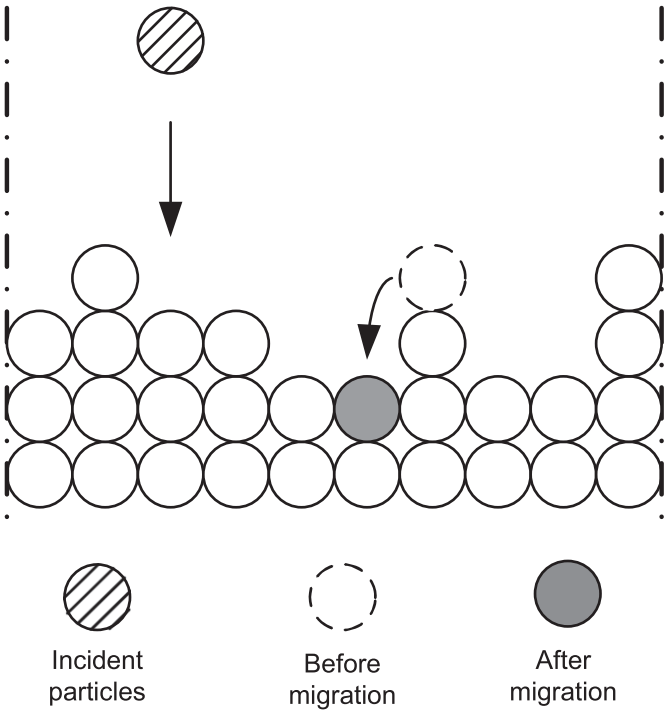

Fig. 3. Thin film growth process on a solid-on-solid one-dimensional square lattice.

After the introduction of the two-stage thin film deposition process, two variables, aggregate RMS surface roughness and slope, are precisely defined to characterize the film aggregate surface morphology which is represented by the aggregate surface height profile. The aggregate RMS surface roughness and aggregate RMS surface slope can be then defined as the root-mean-square of the aggregate surface height profile and the aggregate height slope profile, respectively, as follows:

$$r_{\Delta} = \left[\frac{1}{L/\Delta}\sum_{i=1}^{L/\Delta}(h_{\Delta,i}-\bar{h}_{\Delta})^2\right]^{1/2} \tag{4}$$

$$m_{\Delta} = \left[\frac{1}{L/\Delta}\sum_{i=1}^{L/\Delta}\left(\frac{h_{\Delta,i}-h_{\Delta,i+1}}{\Delta}\right)^2\right]^{1/2} \tag{5}$$

where r_{Δ} denotes the aggregate RMS surface roughness, m_{Δ} denotes the aggregate RMS slope, $h_{\Delta,i}$, $i=1,2,\ldots,L/\Delta$, are the aggregate surface height (with a unit of layer) and $\bar{h}_{\Delta} = (1/L)\sum_{j=1}^{L} h_j$, is the average surface height and L is the lattice size on the lateral direction. Due to the use of PBCs, we have that, $h_{\Delta,(L/\Delta)+1} = h_{\Delta,1}$.

2.2. Spatially distributed deposition rate profile

To improve the performance of the two-stage deposition process, a spatially distributed deposition rate profile is introduced in the second stage of the deposition process (Isabella et al., 2010). Specifically, in the second stage of the deposition process, a spatially distributed deposition rate profile with two sine waves is introduced to carry out the deposition:

$$w(x) = w_0 + A_1 \sin\left(\frac{2\pi k_1 x}{L}\right) + A_2 \sin\left(\frac{2\pi k_2 x}{L}\right) \tag{6}$$

where k_1 and k_2 are the frequencies of the two sine wave functions. It is necessary to note that the amplitude values for both sine wave functions should satisfy $0 \le A_1 + A_2 \le w_0$; this constraint is included to ensure that the deposition rate $w(x)$ is positive everywhere across the film surface.

To explore the properties of this spatially distributed deposition rate profile with multiple sine waves, a series of simulations are carried out at different amplitude values with $k_1 = 5$, $k_2 = 10$, $w_0 = 20$ layer/s, $L=40\,000$ and $A_1 = A_2 = A$ where $A \in [0, 10]$ layer/s. In this series of simulations, the simulation time for the first stage (the stage with uniform deposition rate profile) is zero ($t_{fix} = 0$ s). Fig. 4 shows a snapshot of one of these simulations with $A_1 = A_2 = A = 5$ layer/s. It is clear that the introduction of multiple sine waves changes the shape of the thin film surface and provides more potential to design and control the surface morphology of silicon thin film and improve the performance of thin film solar cells. To further explore its application in improving thin film solar cells, reflectance values are calculated based on Eq. (1) with aggregate roughness and slope values obtained from these simulations; the results are mapped in Fig. 5. R_0 in the plot is the light reflectance of a perfectly smooth surface. Light reflectance of thin films deposited with different A values ($A \in [0, 10]$ layer/s) and spatially distributed deposition rate profiles with ($k_1 = 5$, $k_2 = 0$) and ($k_1 = 0$, $k_2 = 10$) are also mapped in the plot. It is clear that different reflectance values can be generated by utilizing spatially distributed deposition rate profile with multiple sine waves.

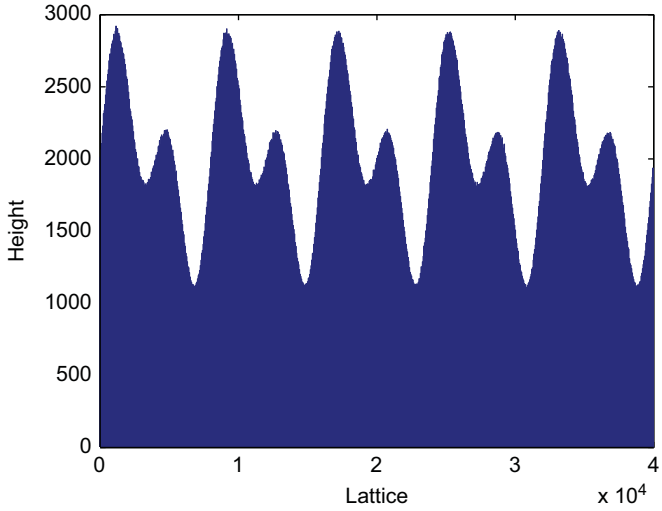

Fig. 4. Snapshot of thin-film with $A_1=A_2=A=5$ layer/s, $k_1=5$, $k_2=10$, $w_0=20$ layer/s and $L=40\,000$.

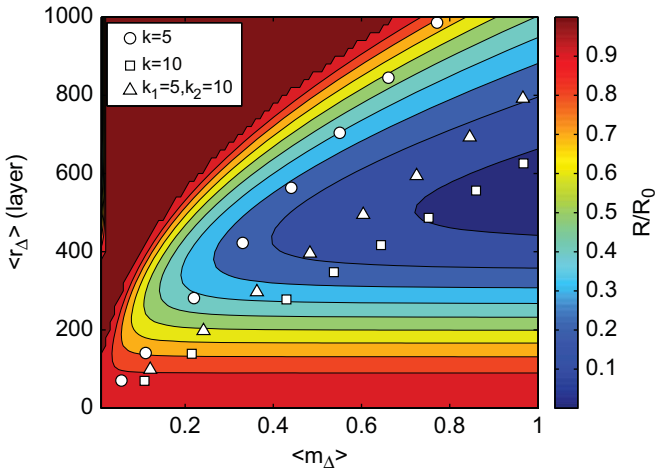

Fig. 5. Light reflectance of thin film deposited with spatially distributed deposition rate profiles of varying complexity with ($k_1=5$, $k_2=0$), ($k_1=0$, $k_2=10$) and ($k_1=5$, $k_2=10$). Circles are results with $k_1=5$ and $k_2=0$; Squares are results with $k_1=0$ and $k_2=10$; Triangles are results with $k_1=5$, $k_2=10$. $A_1=A_2=A$ and $A\in[0,10]$ layer/s.

2.3. Closed-form dynamic model construction

The dynamics and evolution of the aggregate surface height profile, as well as of the aggregate RMS roughness and slope, of the thin film of Fig. 3 can be described by Edwards–Wilkinson (EW)-type equation of the form: Edwards and Wilkinson (1982), Family (1986), and Huang et al. (2011a):

$$\frac{\partial h_{\Delta}}{\partial t}=w(x,t)+c_2\frac{\partial^2 h_{\Delta}}{\partial x^2}+\xi(x,t) \tag{7}$$

subject to the initial condition and the following PBCs:

$$h_{\Delta}(0,t)=h_{\Delta}(L,t),\quad \frac{\partial h_{\Delta}}{\partial x}(0,t)=\frac{\partial h_{\Delta}}{\partial x}(L,t) \tag{8}$$

where $w(x,t)$ is the deposition rate profile. Specifically, in the first stage of the deposition process, $w(x,t)=w_{fix}(t)$ and in the second stage:

$$w(x,t)=w_0(t)+A_1(t)\sin\left(\frac{2\pi k_1 x}{L}\right)+A_2(t)\sin\left(\frac{2\pi k_2 x}{L}\right)$$

where $x\in[0,L]$ is the aggregate spatial coordinate, t is the time, c_2 is the model parameter related to the effect of surface particle migration, and $\xi(x,t)$ is a Gaussian white noise term with a zero mean and a covariance as $\langle\xi(x,t)\xi(x',t')\rangle=\sigma^2\delta(x-x')\delta(t-t')$, where σ^2 is a parameter that measures the noise intensity and $\sigma(\cdot)$ denotes the standard Dirac delta function. These model parameters, c_2 and σ^2, can be estimated on the basis of the kMC simulation data of the thin film deposition process in a least-square sense. It is necessary to note that the initial condition for the first stage of simulation is $h_{\Delta,1}(x,0)=0$ and the initial condition for the second stage of simulation is the final condition of the first stage, $h_{\Delta,2}(x,0)=h_{\Delta,1}(x,t_{fix})$.

To obtain the dynamics of the aggregate RMS roughness and of the aggregate RMS slope, the EW equation is first decomposed into an infinite-dimensional stochastic ODE system as follows (Huang et al., 2011b):

$$\frac{dz_{2,0}}{dt}=w_{2,0}+\xi_{2,0}(t) \tag{9}$$

$$\frac{dz_{p,n}}{dt}=w_{p,n}+\lambda_n z_{p,n}+\xi_{p,n}(t) \tag{10}$$

$$p=1,2,\quad n=1,\ldots,\frac{L}{2\Delta}$$

where λ_n denotes the n-th eigenvalue of the linear second-order operator of Eq. (7), $z_{p,n}(t)$ is the state projection of $h_{\Delta}(x,t)$ in the n-th ODE, and similarly the $\xi_{p,n}$ and $w_{p,n}$ are the projection of noise and $w(x,t)$ on the n-th ODE (Huang et al., 2011b), the value of $w_{p,n}$ is shown as follows:

- If $p=1$,

$$w_{1,n}=\begin{cases}A\sqrt{\frac{L}{2}}, & n=k_1\\ A\sqrt{\frac{L}{2}}, & n=k_2\\ 0 & \text{else}\end{cases} \tag{11}$$

- If $p=2$,

$$w_{2,n}=\begin{cases}0, & n\neq 0\\ A\sqrt{L}, & n=0\end{cases} \tag{12}$$

Since the infinite stochastic ODEs of Eqs. (9) and (10) are linear and uncoupled, the state variance can be directly obtained from the analytical solution of Eqs. (9) and (10) as follows:

$$\langle z_{2,0}(t)\rangle=w_{2,0}(t-t_0) \tag{13}$$

$$var(z_{2,0}(t))=\sigma^2(t-t_0) \tag{14}$$

$$\langle z(t)\rangle=e^{\lambda(t-t_0)}\langle z(t_0)\rangle+\frac{w_p}{\lambda}(e^{\lambda(t-t_0)}-1) \tag{15}$$

$$var(z(t))=e^{2\lambda(t-t_0)}var(z(t_0))+\sigma^2\frac{e^{2\lambda(t-t_0)}-1}{2\lambda} \tag{16}$$

where $z(t)=z_{p,n}(t)$ and $w_p=w_{p,n}$ for $n\neq 0$.

For the purpose of theoretical analysis and control design, the expected value of aggregate RMS roughness square, $\langle r_{\Delta}^2\rangle$, and expected value of aggregate RMS slope square, $\langle m_{\Delta}^2\rangle$, are used in the analysis and controller design later in this work. Both expected aggregate roughness square and expected aggregate slope square can be expressed in terms of state variance, $\langle z_{p,n}^2\rangle$. The derivation can be found in Huang et al. (2011b), and the

results are shown as follows:

$$\langle r_{\Delta}^2(t)\rangle = \frac{1}{L}\sum_{n=1}^{L/(2\Delta)}(\langle z_{1,n}^2\rangle + \langle z_{1,n}^2\rangle) \tag{17}$$

$$\langle m_{\Delta}^2(t)\rangle = \sum_{p=1}^{2}\sum_{n=0}^{L/(2\Delta)} K_{p,n}\langle z_{p,n}^2\rangle \tag{18}$$

where

$$\langle z_{p,n}^2\rangle = var(z_{p,n}) + \langle z_{p,n}\rangle^2 \tag{19}$$

$$K_{p,n} = \frac{8}{L\Delta}\sin^2\left(\frac{\pi n}{L/\Delta}\right)\sum_{i=0}^{L/(2\Delta)}\left(\cos^2\left(\frac{n\pi}{L/\Delta}(2i+1)\right)\right) = \begin{cases}\dfrac{8}{L\Delta}\sin^2\left(\dfrac{\pi n}{L/\Delta}\right) & n=0\\ \dfrac{4}{L\Delta}\sin^2\left(\dfrac{\pi n}{L/\Delta}\right) & n\neq 0\end{cases} \tag{20}$$

It is necessary to point out that, when aggregate (discrete) surface height profile is used, the highest number of modes that can be accurately estimated from $h_{\Delta}(x,t)$ is limited by the spatial sampling points, $n \le L/2\Delta$; the reader may refer to Huang et al. (2011a) for a detailed discussion of the issue.

2.4. Parameter identification and model verification

The model parameters, c_2 and σ^2, of the EW equation of Eq. (7) can be estimated based on the kinetic Monte Carlo simulations results as functions of the mean deposition rate w_0 and/or of the patterned deposition rate magnitudes, A_1 and A_2. These parameters affect the dynamics of aggregate surface roughness and slope and can be estimated by fitting the predicted evolution profiles for aggregate surface roughness and slope from the EW equation to profiles of aggregate surface roughness and slope from kMC simulations. Least-square methods are used to estimate the model parameters so that the EW-model predictions are close in a least-square sense to the kMC simulation data. It is assumed that EW parameters fitted to the kMC results with non-pattern deposition rate profiles can be used to predict the dynamics of kMC simulations with spatially distributed deposition rate profiles; this assumption will be proved to be a valid one in the simulations below. In this work, 40 groups of kMC simulations are carried out from w_0=0.1 layer/s to w_0 = 20 layer/s to compute the dependence of c_2 and σ^2 on w_0. Based on the fitted c_2 and σ^2 values obtained from these fitting results in Figs. 6 and 7, polynomial functions are chosen to estimate c_2 and σ^2 values at different w_0 with the least-square method. Specifically, a second-order polynomial function with respect to w_0 is chosen to estimate c_2 and a linear function is chosen to estimate σ^2, and the expressions are given as follows:

$$c_2(w_0) = a_{c_2}w_0^2 + b_{c_2}w_0 + c_{c_2} \tag{21}$$

$$\sigma^2(w_0) = a_{\sigma^2}w_0 + b_{\sigma^2} \tag{22}$$

where a_{c_2}, b_{c_2}, c_{c_2}, a_{σ^2} and b_{σ^2} are time-invariant fitting model parameters with the following values, $a_{c_2} = -0.0002$, $b_{c_2} = 0.0018$, $c_{c_2} = 0.0007$, $a_{\sigma^2} = 0.9261$ and $b_{\sigma^2} = -0.1168$. These fitting results are based on kMC simulations with uniform deposition rate profiles (A_i=0). To verify that these fittings can be used in the EW equation to predict the open-loop kMC results with spatially distributed deposition rate profiles, the solutions of EW equations for aggregate surface evolution with patterned deposition rate profile are obtained based on c_2 and σ^2 models from open-loop kMC data with uniform deposition rate, and these dynamic evolution profiles are compared with open-loop kMC dynamic evolution profiles with patterned deposition rate profiles. As shown in Figs. 8 and 9, c_2 and σ^2 models from open-loop kMC data with uniform deposition rate can be used in the EW equation to very accurately predict aggregate surface roughness and slope of the kMC model with patterned deposition rate; this conclusion is consistent with Huang et al. (2011b). We note that in the time-scale considered for the deposition (1000 s) both the aggregate surface roughness and slope have not reached their steady-state values and a significantly longer deposition duration is needed for these variables to reach their steady-state values.

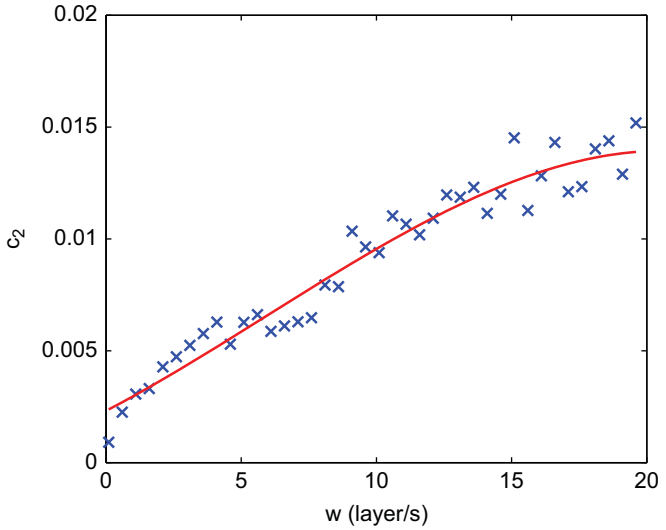

Fig. 6. The c_2 values for different spatially uniform deposition rates $w = w_0$, ($A_1 = A_2 = 0$). The solid line is the result of a second-order polynomial fitting function for the relationship between c_2 and w_0. This relationship is used by the predictive controller.

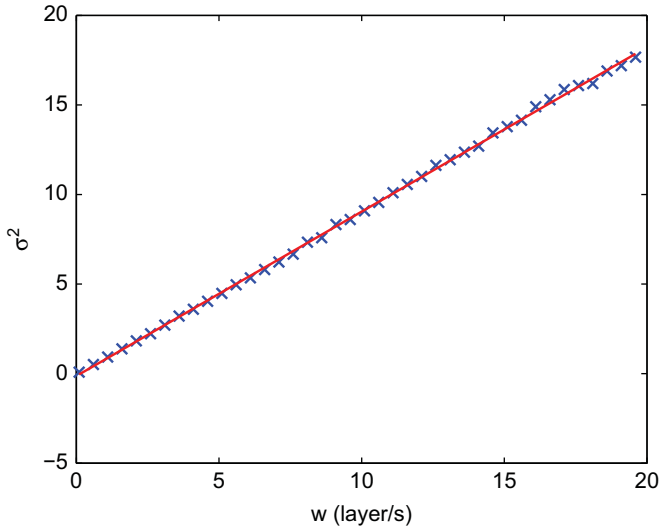

Fig. 7. The σ^2 values for different spatially uniform deposition rates $w = w_0$, ($A_1 = A_2 = 0$). The solid line is the result of a first-order polynomial fitting function for the relationship between σ^2 and w_0. This relationship is used by the predictive controller.

3. Model predictive control

In this section, a model predictive controller is developed on the basis of the constructed closed-form dynamic model. The

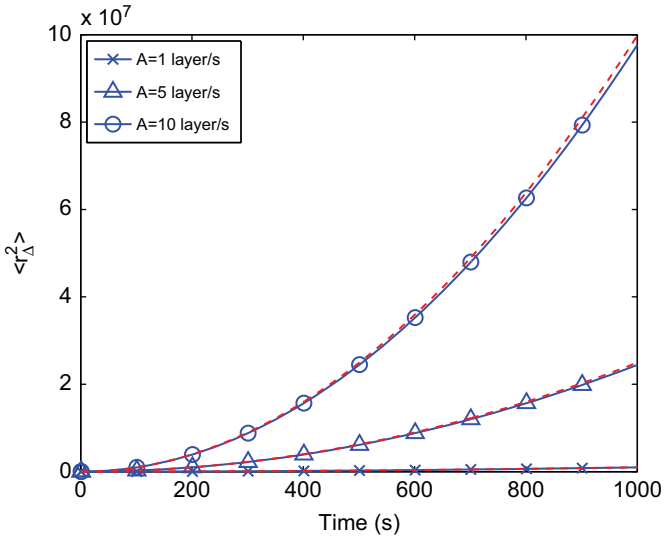

Fig. 8. Evolution of expected aggregate surface roughness for different patterned deposition magnitudes from the kMC model (solid lines with symbols) and expected aggregate surface roughness solutions from the corresponding EW equations (dashed lines, $A_1 = A_2 = A$). The c_2 and σ^2 values of the EW equations were estimated from open-loop aggregate surface roughness kMC model data with spatially uniform deposition rates.

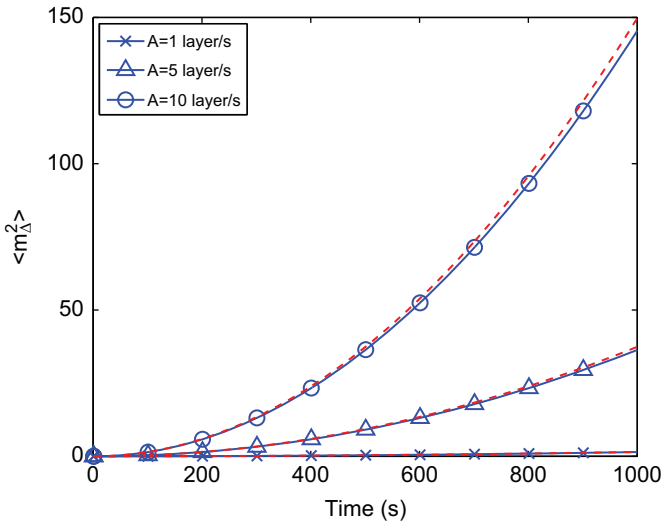

Fig. 9. Evolution of expected aggregate surface slope for different patterned deposition magnitudes from the kMC model (solid lines with symbols) and expected aggregate surface slope solutions from the corresponding EW equations (dashed lines, $A_1 = A_2 = A$). The c_2 and σ^2 values of the EW equations were estimated from open-loop aggregate surface roughness kMC model data with spatially uniform deposition rates.

control objective is to regulate the expected aggregate RMS slope square and the expected aggregate RMS roughness square of the thin film to desired levels.

3.1. MPC formulation

Specifically, we consider the problem of simultaneous regulation of aggregate RMS slope and aggregate RMS roughness of the thin film to desired levels within a model predictive control framework. The expected values of aggregate RMS slope square and of aggregate RMS surface roughness square, $\langle m_\Delta^2 \rangle$ and $\langle r_\Delta^2 \rangle$, are chosen as the control objectives. Since the first stage of the deposition process mainly deals with the thickness of the thin film and the second stage of the process mainly shapes the morphology of the thin film, in this work the control problem focuses mainly on the second stage of the deposition process. The average deposition rate, w_0, and the amplitude of sine wave, A, are used as the manipulated input with a fixed substrate temperature, $T=480$ K. The control action at time t is obtained by solving a finite-horizon optimal control problem. The cost function in the optimal control problem includes penalty on the deviation of $\langle m_\Delta^2 \rangle$ and of $\langle r_\Delta^2 \rangle$ from their set-point values, which are computed to optimize light reflectance of the thin film at desired values. The optimization problem is subject to the dynamics of the aggregate surface height. The manipulated variable profiles are calculated by solving a finite-dimensional optimization problem in a receding horizon fashion. Specifically, the MPC problem is formulated as follows:

$$\min_{(w_0(t_i),A_1(t_i),A_2(t_i))} J = \sum_{i=1}^{p} \{q_m[(m_{\Delta,set}^2 - \langle m_\Delta^2(t_i)\rangle)/m_{\Delta,set}^2]^2 + q_r[(r_{\Delta,set}^2 - \langle r_\Delta^2(t_i)\rangle)/r_{\Delta,set}^2]^2\}$$

s.t.

$$\frac{\partial h_\Delta}{\partial t} = w(x,t) + c_2\frac{\partial^2 h_\Delta}{\partial x^2} + \xi(x,t)$$

$$r_\Delta = \left[\frac{1}{L/\Delta}\sum_{i=1}^{L/\Delta}(h_{\Delta,i} - \bar{h}_\Delta)^2\right]^{1/2}$$

$$m_\Delta = \left[\frac{1}{L/\Delta}\sum_{i=1}^{L/\Delta}\left(\frac{h_{\Delta,i} - h_{\Delta,i+1}}{\Delta}\right)^2\right]^{1/2}$$

$$w_{min} < w_0(t_i) < w_{max}, \quad |w_0(t_i) - w_0(t_i - dt)| \le \delta w_{max}$$

$$w(x,t_i) = w_0(t_i) + A_1(t_i)\sin\left(\frac{2\pi k_1 x}{L}\right) + A_2(t_i)\sin\left(\frac{2\pi k_2 x}{L}\right)$$

$$0 \le A_1(t_i) + A_2(t_i) \le w_0$$

$$i = 1, 2, \ldots, p \qquad (23)$$

where t_i is the current time, dt is the length of the sampling interval, p is the number of prediction steps, $p\,dt$ is the specified prediction horizon, $w_0(t_i)$, $i=1,2,\ldots,p$, is the average deposition rate at the i-th step, q_r and q_m are the weighting penalty factors for the deviations of $\langle m_\Delta^2 \rangle$ and $\langle r_\Delta^2 \rangle$ from their respective set-points, $r_{\Delta,set}^2$ and $m_{\Delta,set}^2$, at the i-th prediction step, w_{min} and w_{max} are the lower and upper bounds on the average deposition rate, respectively, and δw_{max} is the limit on the rate of change of the average deposition rate. It is necessary to note that several constraints are added to the controller to account for a number of practical considerations. First, there is a constraint on the range of variation of the average deposition rate. Another constraint is imposed on the rate of change of the average deposition rate to account for actuator limitations. The optimal manipulated variable profile, $(w_0(t_i), A(t_i))$, is obtained from the solution of the optimization problem of Eqs. (23), which minimizes the deviation of the expected aggregate RMS slope square and of the expected aggregate RMS roughness square from their respective set-point values within the prediction horizon.

The surface aggregate RMS roughness square and slope square can be calculated in terms of the state variance, as is shown in Eqs. (17) and (18), then the MPC formulation can be modified as follows:

$$\min_{(w_0(t_i),A_1(t_i),A_2(t_i))} J = \sum_{i=1}^{p} \{q_m[(m_{\Delta,set}^2 - \langle m_\Delta^2(t_i)\rangle)/m_{\Delta,set}^2]^2 + q_r[(r_{\Delta,set}^2 - \langle r_\Delta^2(t_i)\rangle)/r_{\Delta,set}^2]^2\}$$

s.t.

$$\langle r_\Delta^2(t)\rangle = \frac{1}{L}\sum_{n=1}^{L/(2\Delta)}(\langle z_{1,n}^2\rangle + \langle z_{1,n}^2\rangle)$$

$$\langle m_{\Delta}^2(t)\rangle = \sum_{p=1}^{2}\sum_{n=0}^{L/(2\Delta)} K_{p,n}\langle z_{p,n}^2\rangle$$
$$w_{min} < w_0(t_i) < w_{max}, \quad |w_0(t_i) - w_0(t_i - dt)| \le \delta w_{max}$$
$$w(x,t_i) = w_0(t_i) + A_1(t_i)\sin\left(\frac{2\pi k_1 x}{L}\right) + A_2(t_i)\sin\left(\frac{2\pi k_2 x}{L}\right)$$
$$0 \le A_1(t_i) + A_2(t_i) \le w_0$$
$$i = 1, 2, \ldots, p \qquad (24)$$

4. Regulation of surface slope and roughness for light trapping efficiency

In this section, we apply the predictive controller of Eqs. (24) to the kMC model of the thin film deposition process to regulate the surface aggregate slope and roughness at desired levels. The average deposition rate and amplitude of sine waves are chosen as manipulated variables. The substrate temperature is kept constant during all deposition runs. The controlled variables are the expected values of the aggregate RMS slope square and of the aggregate RMS roughness square at the end of the deposition process.

In the closed-loop simulations, the aggregate surface height profile of the thin film is obtained from the kMC simulations and is transferred to the controller (state feedback control) at each sampling time; the sampling time is $dt = 5$ s and the time needed to solve the MPC problem at each sampling time ranges from 1 to 3 s. Furthermore, the prediction horizon $p\,dt$ is chosen to be the length of time between the current sampling time and the entire deposition duration (t_f) owing to the batch nature of the deposition process. A finite number of modes, $L/(2\Delta)$, are reconstructed from the aggregate surface height profile and are used to calculate the predictions of the aggregate RMS slope square and of the aggregate RMS roughness square. The constrained optimization problem formulated in the MPC of Eqs. (24) is solved and the optimal input profile is obtained and is applied to the closed-loop system during the sampling time. The optimization problem is solved via a local constrained minimization algorithm with a broad set of initial guesses.

4.1. Surface regulation of two-stage deposition process with $k_1 = 5$, $k_2 = 0$ and $A_1 = A_2 = A$

In this subsection, several groups of set-points are picked to generate thin-film surfaces corresponding to different light reflectance values, $R/R_0 = 0.2$, $R/R_0 = 0.5$ and $R/R_0 = 0.9$. In the first stage of the simulation, open-loop simulations are carried out with $w_{fix} = 10$ layer/s and simulation time is $t_{fix} = 5000$ s. In the second stage of the simulation, closed-loop simulations are carried out at different set-points with fixed weighting factors on roughness and slope of $q_r = q_m = 1$ and $A_1 = A_2 = A$. The obtained aggregate roughness and slope are substituted into Eq. (1) to calculate the corresponding reflectance value. Specifically, in the first group of simulations, $m_{\Delta,set}^2 = 0.16$ and $r_{\Delta,set}^2 = 160\,000$ layer^2/s, and the results are shown in Fig. 10. It is clear in the plot that during the first stage of simulation ($t_{fix} = 5000$ s), aggregate surface roughness and slope increase very slowly and both variables increase fast and approach set-points during the second stage of the deposition. This is as expected because the amplitude value, A, is the key factor to shape the morphology of the thin film surface during the second stage of the deposition. Larger deviation from the set-point is observed for the aggregate slope than for the aggregate roughness. This is determined by the ratio between the weighting factors and more details can be found in Huang et al. (2011b); specifically, when

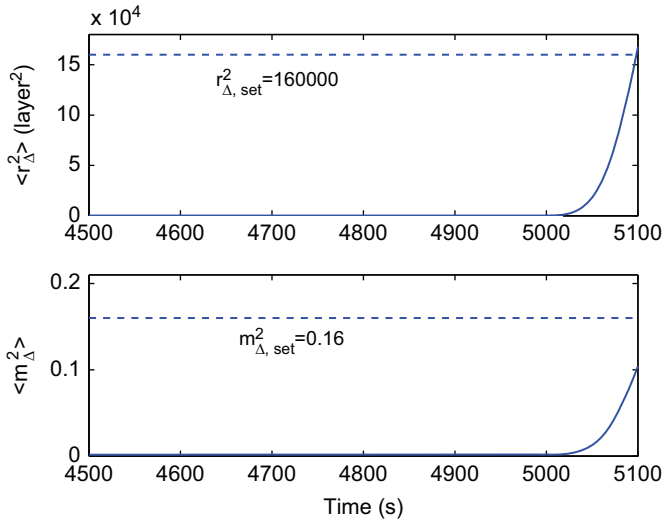

Fig. 10. $\langle r_{\Delta}^2\rangle$ and $\langle m_{\Delta}^2\rangle$ profiles of the closed-loop thin film deposition with $k_1 = 5$ and $k_2 = 0$ corresponding to light reflectance value $R/R_0 = 0.2$ with $q_r = q_m = 1$, $r_{\Delta,set}^2 = 160\,000$ layer^2, $m_{\Delta,set}^2 = 0.16$ and $A_1 = A_2 = A$.

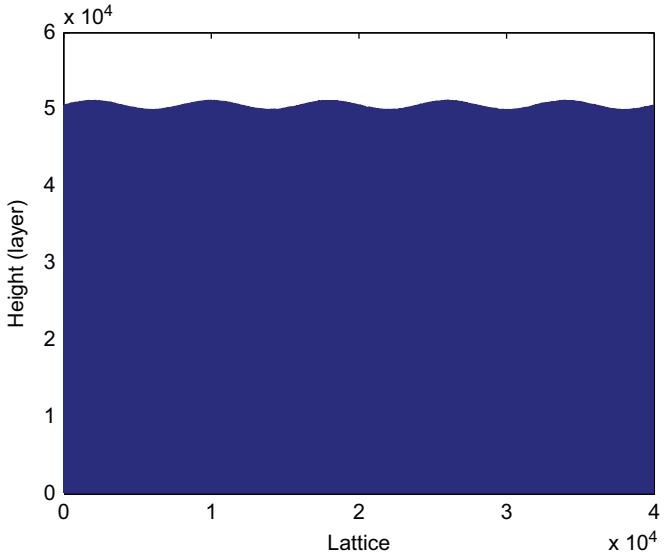

Fig. 11. Surface snapshot for closed-loop thin film deposition using actuation with $k_1 = 5$ and $k_2 = 0$ corresponding to light reflectance value $R/R_0 = 0.2$ and $A_1 = A_2 = A$.

the ratio (q_r/q_m) is small, the aggregate slope approaches its set-point value at the expense of a significant deviation of the aggregate roughness from its set-point, and vice-versa. The light reflectance value with the obtained aggregate roughness and slope is $R/R_0 = 0.24$, which is close to the desired value. The surface snapshot in this case is shown in Fig. 11 and a clear pattern can be observed on the thin film surface.

Similarly, simulations are carried out to generate surfaces with $R/R_0 = 0.5$ and $R/R_0 = 0.9$ and the resulting surface snapshots are shown in Figs. 12 and 13. The obtained light reflectance values in these two cases are $R/R_0 = 0.54$ and $R/R_0 = 0.89$, respectively, both of which are close to the desired values. As the surface becomes smoother, the light reflectance value approaches the reflectance for perfectly smooth surface, where $R = R_0$.

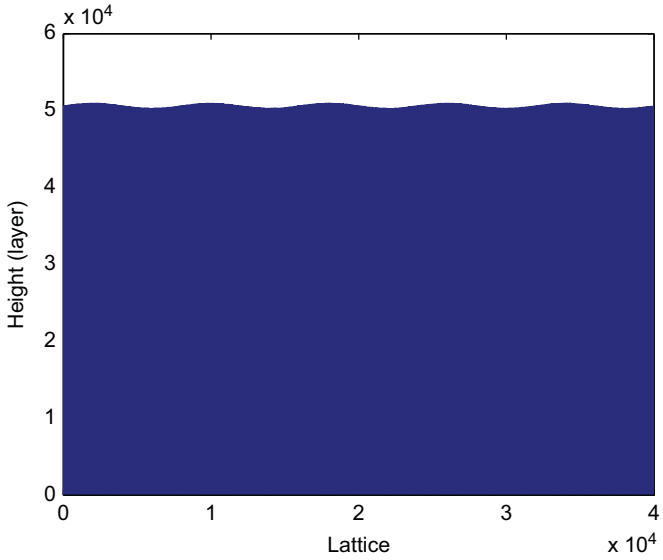

Fig. 12. Surface snapshot for closed-loop thin film deposition using actuation with $k_1=5$ and $k_2=0$ corresponding to light reflectance value $R/R_0=0.5$ and $A_1=A_2=A$.

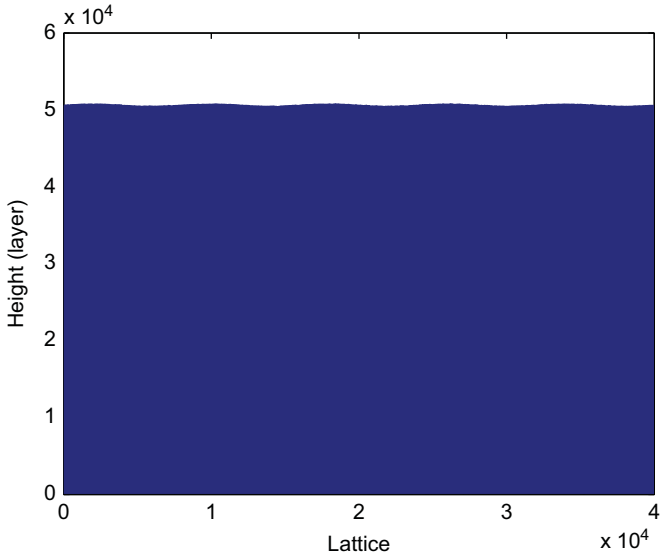

Fig. 13. Surface snapshot for closed-loop thin film deposition using actuation with $k_1=5$ and $k_2=0$ corresponding to light reflectance value $R/R_0=0.9$ and $A_1=A_2=A$.

4.2. Separate control of aggregate surface roughness and slope for two-stage deposition process with $k_1=5$, $k_2=10$ and $A_1=A_2=A$

In this subsection, the two-stage kMC simulation model is replaced with the one which utilizes a spatially distributed deposition rate profile with multiple sine waves. To focus on the regulation of aggregate surface roughness and slope in the second stage of simulations, in this subsection the simulation time for the first stage of simulation is set to be short, $t_{fix}=10$ s. In the second stage of simulations, multiple frequencies $k_1=5$ and $k_2=10$ are used. First, the problem of regulating aggregate surface roughness is considered. In this problem, the cost function has only penalty on the deviation of the expected aggregate surface roughness square from its set-point, i.e., $q_r=1$, $q_m=0$ and $A_1=A_2=A$. The set-point, $r^2_{\Delta,set}$ is 10 000 layer^2. Fig. 14 shows the evolution profile of $\langle r^2_\Delta \rangle$ under the model predictive

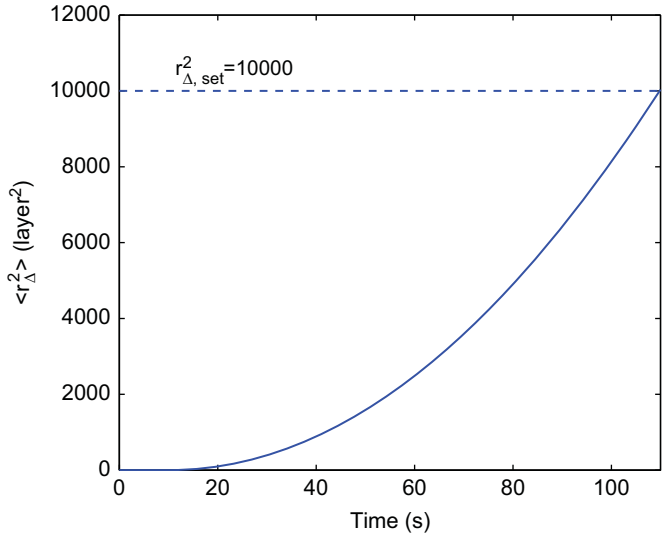

Fig. 14. Profile of expected aggregate surface roughness square with $k_1=5$ and $k_2=10$. $q_r=1$, $q_m=0$, $r^2_{\Delta,set}=10\,000$ layer^2 and $A_1=A_2=A$.

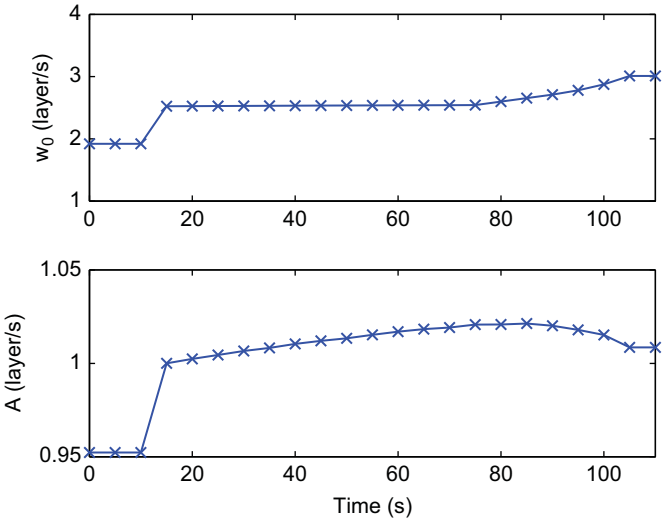

Fig. 15. Manipulated input profiles with $k_1=5$ and $k_2=10$. $q_r=1$, $q_m=0$, $r^2_{\Delta,set}=10\,000$ layer^2 and $A_1=A_2=A$.

controller of Eq. (24). It is clear that the controller drives the expected aggregate surface roughness to its set-point at the end of the simulation (110 s). Fig. 15 shows the input profiles of w_0 and A for these simulations.

Next, the aggregate surface slope is regulated. The cost function includes only penalty on the deviation of the expected value of aggregate surface slope square from its set-point ($q_m=1$, $q_r=0$). The set-point, $m^2_{\Delta,set}$ is 0.25. Fig. 16 shows the evolution profile of the expected aggregate slope square. The aggregate slope reaches its set-point at $t=110$ s. Fig. 17 displays the input profile in this scenario. It is necessary to point out that during the first half of the simulation time, the optimal solutions of w_0 are constrained by the rate of change constraint and the optimal solutions of A are bounded by the values of w_0.

4.3. Surface regulation of two-stage deposition process with $k_1=5$, $k_2=10$ and $A_1=A_2=A$

In this subsection, the kMC simulation model with a spatially distributed deposition rate profile with multiple sine waves is still

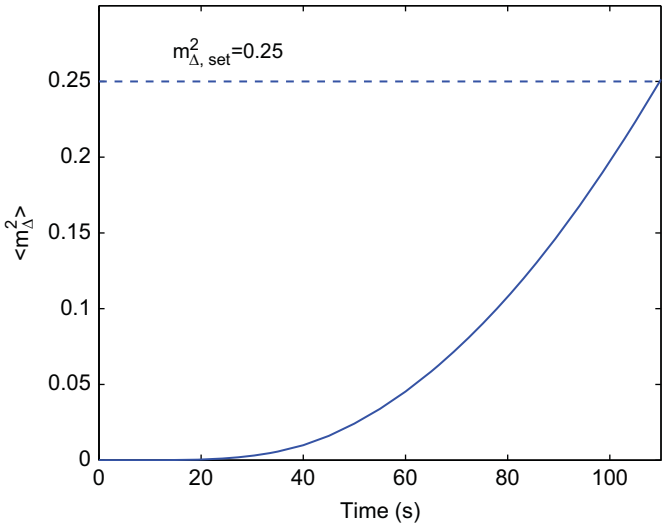

Fig. 16. Profile of expected aggregate surface slope square with $k_1 = 5$ and $k_2 = 10$. q_r=0, q_m=1, $m^2_{\Delta,set} = 0.25$ and $A_1 = A_2 = A$.

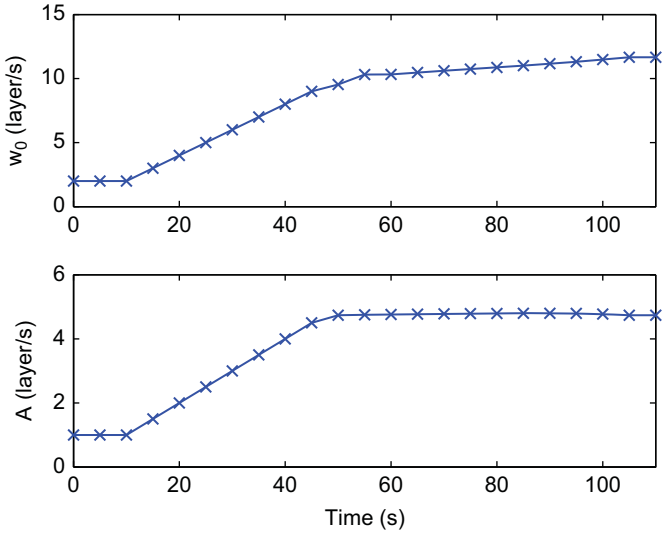

Fig. 17. Manipulated input profiles with $k_1 = 5$ and $k_2 = 10$. q_r=0, q_m=1, $m^2_{\Delta,set} = 0.25$ and $A_1 = A_2 = A$.

utilized to carry out the simulation, but different from the previous part, the cost function in this subsection has penalties on both aggregate roughness and aggregate slope. The set-points $m^2_{\Delta,set} = 0.25$ and $r^2_{\Delta,set} = 160\,000$ layer^2/s are used. The closed-loop simulation results are shown in Fig. 18 and the obtained aggregate roughness and slope generates a surface with light reflectance value $R/R_0 = 0.21$, which is very close to the desired value. The resulting final surface snapshot is shown in Fig. 19. It is important to point out that in the closed-loop simulations in this work, all the set-points are reached with $0 \le A \le 10$ layer/s, which means that the fitting used in this work is valid for all the set-points.

4.4. *Surface regulation of two-stage deposition process with $k_1 = 5$, $k_2 = 10$ and $A_1 \neq A_2$*

Similar to the previous subsection, the kMC model with $k_1 = 5$ and $k_2 = 10$ is utilized, but A_1 and A_2 are allowed to be adjusted independently by the controller. Specifically, the MPC has three manipulated variables, w_0, A_1 and A_2, all of which can change

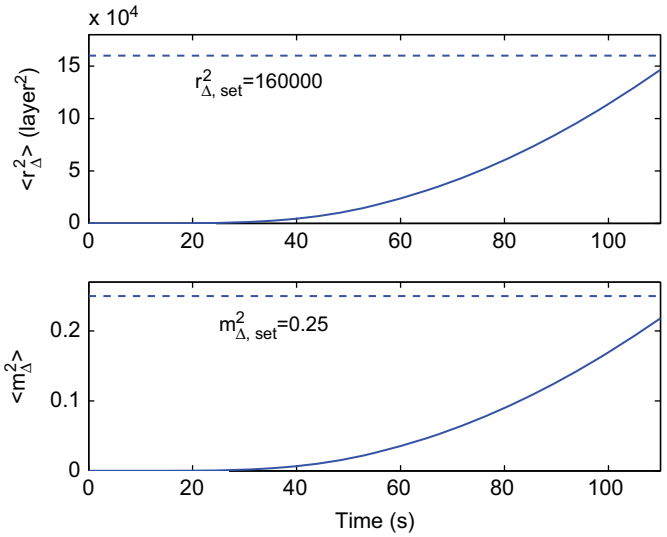

Fig. 18. $\langle r^2_\Delta \rangle$ and $\langle m^2_\Delta \rangle$ profiles of the closed-loop thin film deposition with $k_1 = 5$ and $k_2 = 10$ corresponding to light reflectance value $R/R_0 = 0.2$ with $q_r = q_m = 1$, $r^2_{\Delta,set} = 160\,000$ layer^2, $m^2_{\Delta,set} = 0.25$ and $A_1 = A_2 = A$.

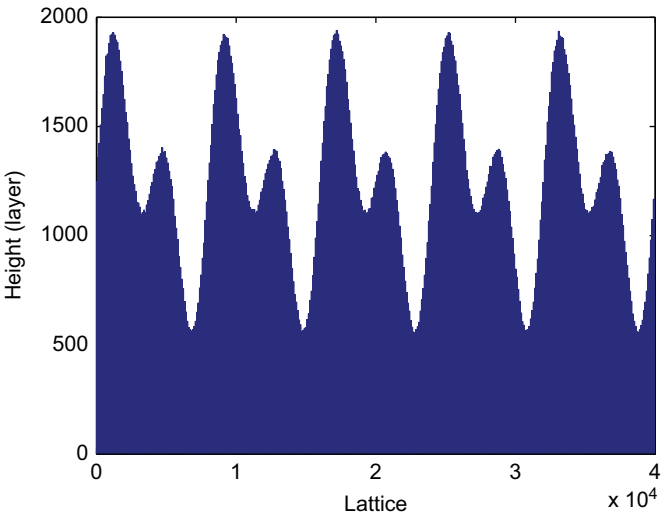

Fig. 19. Surface snapshot for closed-loop thin film deposition using actuation with $k_1 = 5$ and $k_2 = 10$ corresponding to light reflectance value $R/R_0 = 0.2$ and $A_1 = A_2 = A$.

independently. The set-points $m^2_{\Delta,set} = 0.25$ and $r^2_{\Delta,set} = 160\,000$ layer^2/s are used. The closed-loop simulation results are shown in Fig. 20. It is clear that both $\langle r^2_\Delta \rangle$ and $\langle m^2_\Delta \rangle$ reach their set-points at the end of the closed-loop simulation. The ability to independently vary w_0, A_1 and A_2 makes it possible to reach the set-points for both aggregate roughness and slope at the same time and substantially improve the performance of the MPC. Fig. 21 shows the input profiles of w_0, A_1 and A_2 for the simulation and the corresponding final thin film surface snapshot is shown in Fig. 22.

5. Conclusions

A model predictive control algorithm was developed to regulate the aggregate surface slope and roughness of a two-stage thin film growth process. The two-stage thin film deposition process, which is characterized by a stage with uniform deposition rate profile and a stage with spatially distributed deposition rate profile, was modeled on a one-dimensional solid-on-solid

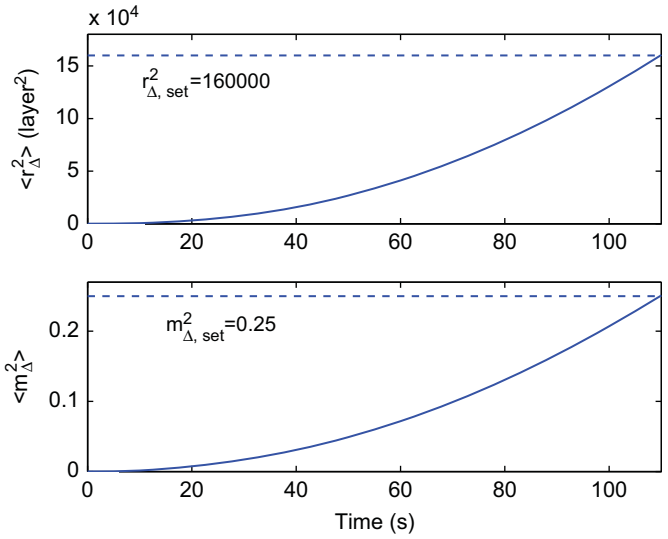

Fig. 20. $\langle r_{\Delta}^2 \rangle$ and $\langle m_{\Delta}^2 \rangle$ profiles of the closed-loop thin film deposition with $k_1 = 5$ and $k_2 = 10$ corresponding to light reflectance value $R/R_0 = 0.2$ with $q_r = q_m = 1$, $r_{\Delta,set}^2 = 160\,000$ layer^2 and $m_{\Delta,set}^2 = 0.25$.

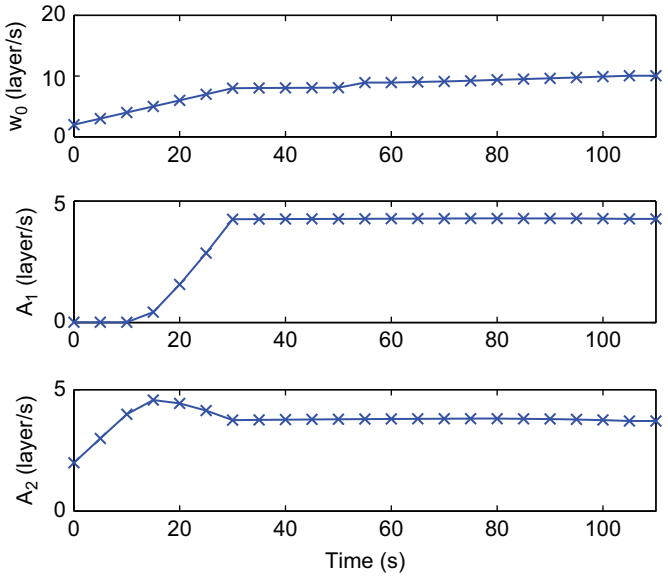

Fig. 21. Manipulated input profiles with $k_1 = 5$ and $k_2 = 10$. The $q_r = q_m = 1$, $r_{\Delta,set}^2 = 160\,000$ layer^2 and $m_{\Delta,set}^2 = 0.25$.

square lattice that involves two microscopic processes: an adsorption process and a migration process. Kinetic Monte Carlo methods were used to simulate the two-stage thin film deposition process and the spatially distributed deposition rate profile with single or multiple sine waves were introduced to carry out the two-stage thin film deposition process. To characterize the surface morphology and to evaluate the light trapping efficiency of the thin film, aggregate surface roughness and aggregate surface slope were introduced as the root-mean squares of the aggregate surface height profile and aggregate surface slope profile. An EW-type equation was used to describe the dynamics of the aggregate surface height profile and predict the evolution of the aggregate RMS roughness and aggregate RMS slope. The model parameters of the EW equation were estimated from simulation data through least-square methods. A model predictive control algorithm was then developed on the basis of the EW equation model to

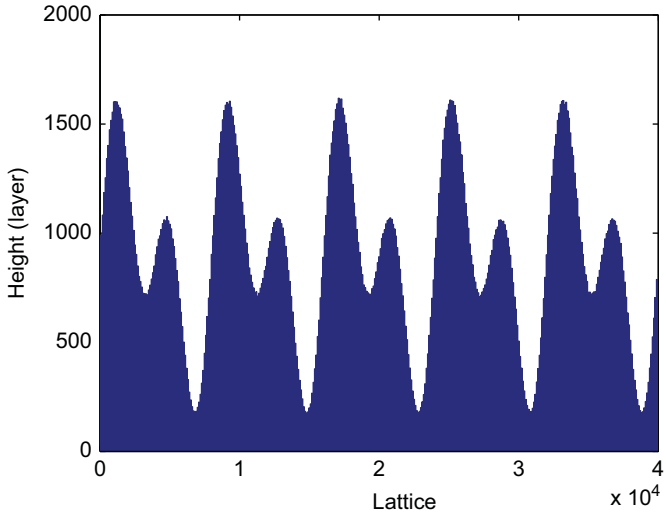

Fig. 22. Surface snapshot for closed-loop thin film deposition using actuation with $k_1 = 5$ and $k_2 = 10$.

simultaneously regulate the aggregate RMS slope and the aggregate RMS roughness at desired levels by optimizing average deposition rates and amplitude values in the second stage of the deposition at each sampling time. Closed-loop simulation results were presented to demonstrate the effectiveness of the proposed model predictive control algorithm in successfully regulating the aggregate RMS slope and the aggregate RMS roughness at desired levels that generate desired thin film light reflectance and transmittance.

References

Bennett, H.E., Porteus, J.O., 1961. Relation between surface roughness and specular reflectance at normal incidence. J. Opt. Soc. Am. 51, 123–129.
Christofides, P.D., Armaou, A., Lou, Y., Varshney, A., 2008. Control and Optimization of Multiscale Process Systems. Birkhäuser, Boston.
Davies, H., 1954. The reflection of electromagnetic waves from a rough surface. Proc. Inst. Electr. Eng. 101, 209.
Edwards, S.F., Wilkinson, D.R., 1982. The surface statistics of a granular aggregate. Proc. R. Soc. London Ser. A – Math. Phys. Eng. Sci. 381, 17–31.
Family, F., 1986. Scaling of rough surfaces: effects of surface diffusion. J. Phys. A: Math. Gen. 19, L441–L446.
Hu, G., Orkoulas, G., Christofides, P.D., 2009. Regulation of film thickness, surface roughness and porosity in thin film growth using deposition rate. Chem. Eng. Sci. 64, 3903–3913.
Huang, J., Hu, G., Orkoulas, G., Christofides, P.D., 2011a. Dynamics and lattice-size dependence of surface mean slope in thin film deposition. Ind. Eng. Chem. Res. 50, 1219–1230.
Huang, J., Zhang, X., Orkoulas, J., Christofides, P.D., 2011b. Dynamics and control of aggregate thin film surface morphology for improved light trapping: implementation on a large-lattice kinetic monte carlo model. Chem. Eng. Sci. 66, 5955–5967.
Isabella, O., Krč, J., Zeman, M., 2010. Modulated surface textures for enhanced light trapping in thin-film silicon solar cells. Appl. Phys. Lett. 97, 101–106.
Krč, J., Smole, F., Topič, M., 2003. Analysis of light scattering in amorphous Si: H solar cells by a one-dimensional semi-coherent optical model. Prog. Photovolt.: Res. Appl. 11, 15–26.
Krč, J., Zeman, M., 2002. Experimental investigation and modelling of light scattering in α-Si : H solar cells deposited on glass/ZnO:Al substrates. Mater. Res. Soc. Proc. 715.
Leblanc, F., Perrin, J., 1994. Numerical modeling of the optical properties of hydrogenated amorphous-silicon-based P–I–N solar cells deposited on rough transparent conducting oxide substrates. J. Appl. Phys. 75, 1074.
Levine, S.W., Clancy, P., 2000. A simple model for the growth of polycrystalline Si using the kinetic Monte Carlo simulation. Model. Simulat. Mater. Sci. Eng. 8, 751–762.
Levine, S.W., Engstrom, J.R., Clancy, P., 1998. A kinetic Monte Carlo study of the growth of Si on Si(100) at varying angles of incident deposition. Surf. Sci. 401, 112–123.
Müller, J., Rech, B., Springer, J., Vanecek, M., 2004. TCO and light trapping in silicon thin film solar cells. Solar Energy 77, 917–930.
Poruba, A., Fejfar, A., 2000. Optical absorption and light scattering in microcrystalline silicon thin films and solar cells. J. Appl. Phys. 88, 148–160.

Rowlands, S.F., Livingstone, J., Lund, C.P., 2004. Optical modelling of thin film solar cells with textured interfaces using the effective medium approximation. Solar Energy 76, 301–307.

Springer, J., Poruba, A., 2004. Improved three-dimensional optical model for thin-film silicon solar cells. J. Appl. Phys. 96, 5329–5337.

Tao, G., Zeman, M., 1994. Optical modeling of α-Si : H based solar cells on textured substrates. In: 1994 IEEE First World Conference on Photovoltaic Energy Conversion. Conference Record of the Twenty Fourth IEEE Photovoltaic Specialists Conference – 1994 (Cat.No.94CH3365-4), 1, 666.

Wang, L., Clancy, P., 2001. Kinetic Monte Carlo simulation of the growth of polycrystalline Cu films. Surf. Sci. 473, 25–38.

Yang, Y.G., Johnson, R.A., Wadley, H.N.G., 1997. A Monte Carlo simulation of the physical vapor deposition of nickel. Acta Mater. 45, 1455–1468.

Zeman, M., Vanswaaij, R., 2000. Optical modeling of a-Si: H solar cells with rough interfaces: effect of back contact and interface roughness. J. Appl. Phys. 88, 6436–6443.

Zhang, P., Zheng, X., Wu, S., Liu, J., He, D., 2004. Kinetic Monte Carlo simulation of Cu thin film growth. Vacuum 72, 405–410.

Zhang, X., Huang, J., Orkoulas, G., Christofides, P.D., 2012. Controlling aggregate thin film surface morphology for improved light trapping using a patterned deposition rate profile. Chem. Eng. Sci. 67, 101–110.